التحليل الموسمي للعلاقة بين درجة حرارة سطح الأرض وديناميكيات رطوبة السطح على أغطية أرضية متنوعة: إدارة گرميان كدراسة حالة

د. هيمن نصرالدين محمد أمين

قسم الجغرافيا، كلية التربية، جامعة گرميان، إقليم كوردستان – العراق.

hemin.nasraldin@garmian.edu.krd

د. هيرو نصرالدين محمد أمين

قسم الجغرافيا، كلية العلوم الإنسانية، جامعة السليمانية، إقليم كوردستان – العراق.

hero.mohammedamin@univsul.edu.iq

م. عثمان عبد الرحمن علي

قسم العلوم الاجتماعية، كلية التربية الأساسية، جامعة گرميان، إقليم كوردستان – العراق.

othman.abdulrhman@garmian.edu.krd

Seasonal Analysis of the Correlation Between Land Surface Temperature and Surface Moisture Dynamics on Various Land Covers; Garmian Administration as a Case Study

Dr. Hemin Nasraldin M. Amin

Department of Geography, College of Education, University of Garmian, Kurdistan Region – Iraq.

Dr. Hero Nasraldin M. Amin

Department of Geography, College of Humanities, University of Sulaimani, Kurdistan Region – Iraq.

L. Othman Abdulrhman Ali

Department of Social Sciences, College of Basic Education, University of Garmian, Kurdistan Region– Iraq.

المستخلص

هدفت هذه الدراسة إلى تحليل العلاقة الارتباطية بين درجة حرارة سطح ومؤشر اختلاف المائية المعياري المعدل (MNDWI) على أسطح أرضية متنوعة تختلف من حيث مستويات الرطوبة. تم اختيار إدارة گرميان كدراسة حالة، وهي تقع في الجنوب الشرقي من إقليم كوردستان العراق ضمن منطقة شبه جافة. تم استخراج بيانات درجة حرارة سطح الأرض باستخدام خوارزمية النافذة الاحادية (Mono-Window Algorithm) لمجموعة من مرئيات القمر الصناعي (Landsat) التي تم الحصول عليها للفصول الأربعة من عام ٢٠٢٥. كما استُخدمت المرئية (Landsat true color) وخريطة الأساس من نظم المعلومات الجغرافي (GIS) إلى جانب مؤشر (MNDWI) لتحديد أنواع الغطاء الأرضي المختلفة بناءً على الرطوبة. واستُخدم معامل ارتباط بيرسون لتفسير تأثير المسطحات المائية والمناطق الرطبة على درجة حرارة سطح الأرض. أظهرت النتائج أن طبيعة تأثير مؤشر (MNDWI) على درجة حرارة سطح الأرض تختلف باختلاف الفصول والأسطح، حيث لوحظ أقوى ارتباط رطوبي في المسطحات المائية. وسجلت المسطحات المائية في فصل الخريف أقوى ارتباط سلبي (r = -0.82) ، بينما سجلت في فصل الشتاء أقل ارتباط (r = -0.17) ، حيث قد يكون لعوامل أخرى تأثير أكبر من الرطوبة في هذا الفصل. تخلص الدراسة إلى أن مؤشر(MNDWI) يعد نهجاً موثوقاً لمراقبة ديناميكيات درجة الحرارة في منطقة گرميان، نظراً لأن معظم النتائج كانت ذات دلالة إحصائية (p < 0.01).

الكلمات المفتاحية : درجة حرارة سطح الأرض(LST) ، مؤشر اختلاف المائية المعياري المعدل (MNDWI) ، معامل ارتباط بيرسون، إدارة گرميان.

Abstract

This study aimed to examine the correlation between Land Surface Temperature (LST) and Modified Normalized Differences Vegetation Index (MNDWI) on different wetness-based land surfaces, Garmian Administration is selected as a case study, it is located in southeast of Iraqi Kurdistan region in semi-arid region. LST retrieved using Mono-Window Algorithm for a set of Landsat images acquired for the four seasons of 2025. Landsat True color and GIS base map along with MNDWI index were used to determine various wetness-based land cover types, the Pearson correlation coefficient was used to explain the impact of water body and wetness areas on LST. Results show that the nature of MNDWI impact on LST is different in each seasons and surfaces, the greatest and wettest association was noticed in water bodies. Autumn water bodies had the strongest negative correlation (r=-0.82), while Winter water bodies have the smallest (r=-0.17), where other factors may play a greater influence than wetness. MNDWI is a reliable approach for monitoring temperature dynamics in the Garmian area, since most results were statistically significant (p < 0.01).

Keyword: LST, MNDWI, Pearson Correlation Coefficient, Garmian Administration

بسم الله الرحمن الرحيم

1. Introduction:

Land surface temperature (LST) is a critical parameter in monitoring the biogeochemical processes on the land surface. LST varies depending on land surface structure. It is often low in green vegetation and water bodies, but high in built-up areas, exposed rock surfaces, and dry soil (Guha & Govil, 2021). The LSTs of water bodies are often lower. As a result, a better knowledge of the effects of impermeable surfaces and green infrastructure on LST is required for minimizing negative consequences and aiding urban planning and public health management (Ge et al., 2020). Correlation analyses between spectral indices and LST in various cities have been reported in a number of recent publications that are pertinent to this investigation (Pearsall, 2017, (Amin & Ahmad, 2024), Zhang et al., 2026). Several studies have examined the correlation between the moisture land covers and Land Surface Temperature (LST) in several areas and ecosystems (Chanyal & Purohit, 2024, Guha & Govil, 2021). In semi-arid regions, landscape modification and the decrease of natural moisture surfaces have been proven to generate dramatic rises in LST (Ali et al., 2025).The thermal environment and geographical information can be effectively analyzed using remote sensing images with several resolutions and temporal scales. High-resolution data necessary for simulating these spatiotemporal temperature dynamics are provided by recent developments in Landsat 8 and 9 photography (Grigoras & Uritescu, 2024). This study seeks to completely assess the association between LST and moisture conditions in the Garmian administration, to evaluate thermal characteristics of different moisture surfaces across seasons using LST and MNDWI derived from Landsat satellite data.

2. Materials and Methods

2.1. Study Area

The Garmian Administration is located in a sub-mountainous area in both northeastern Iraq and the southeast of the Kurdistan Region. The Garmian Administration is 6,017.95 km^2 in total. It includes the sub-districts of Maidan and Qoratu (which are administratively a part of the Khanaqin district) and the districts of Kalar, Rizgari and Kifri. Astronomically, the region is located between latitudes 34˚ 05' 10" - 35˚ 05' 26" North, and longitudes 44˚ 29' 10" - 45˚ 48' 15" East (Fig.1). According to Buday & Jassim's (1984) tectonic classification, the Garmian Administration is situated on the Foothill Zone of the Unstable Shelf. As a transitional zone between the southern alluvial plains and the northern/northeastern mountainous highlands, the area is a part of the Kurdistan Region's sub-mountainous region. From 128 meters above sea level in the southern reaches to 1,832 meters at the summit of Bamo mountain in the northeast, elevation progressively rises from south to north.

According to the Köppen (1936) The majority of the area is classified as having a semi-arid climate (Bsh). Seasonal shifts and topographical diversity result in significant seasonal and spatial variations in climatic elements. In terms of soil, the study area's soil types include Brown, Reddish-Brown, Lithosol, and Grumusol (cracking soil), according to Buringh (1960). Furthermore, the plains of Sherwana and Shakal, as well as the banks of the Sirwan River, have rich alluvial soils that make them ideal for agriculture, especially grain farming. There are three types of natural vegetation that have adapted to the local climate: Mountain Forests, which are found on the highest altitude slopes in the north. The Sirwan River and its permanent tributaries are home to riverine forests. Steppe Vegetation: From mid-winter to

late spring, the majority of the area is covered by short grasses, or steppes. In terms of water resources, the Sirwan River and its tributaries (Hawasan, Qoratu, and Awaspi) are permanent sources in the study area. There are many ponds (Ali Mir, Tanura, Razwar, Bestana, Robitan, Aubara, and Mlasura) as well as several dams (Bawashaswar, Khornawazan, and Awaspi).

Figure 1. Location Map of the Study area

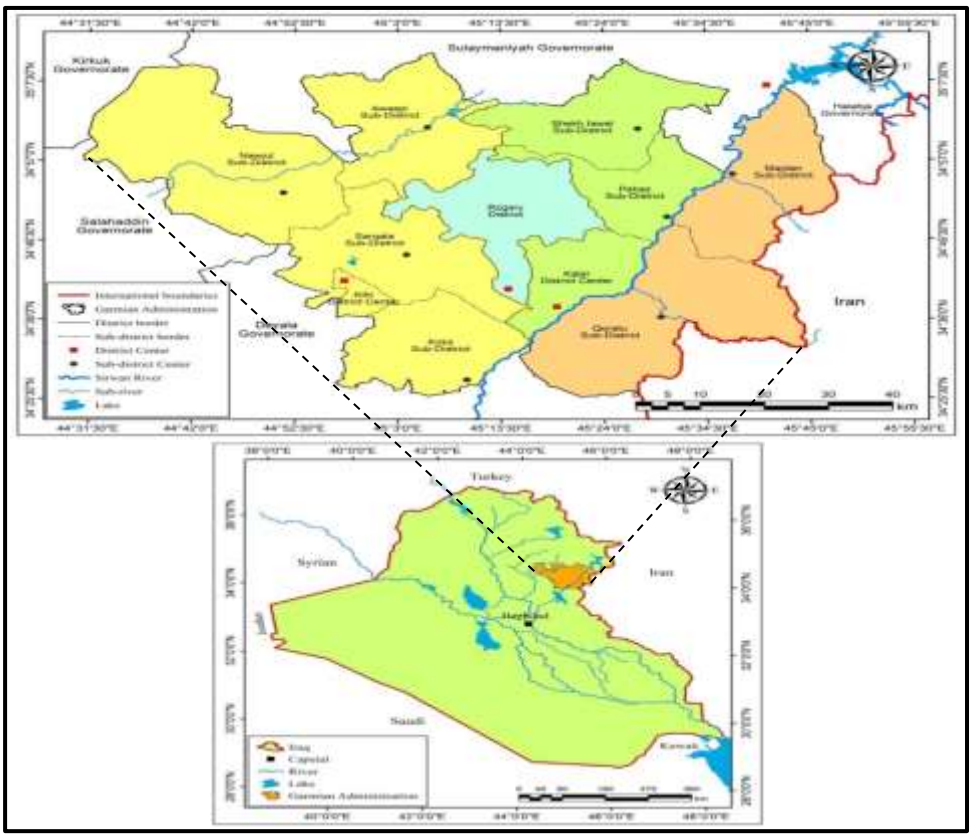

The map prepared using ArcGIS 10.8.1 based on data from the Garmian Administration Technical Department and the Sulaymaniyah Statistical Administration (2022).

2.2. Dataset and Software used

Four Landsat images were obtained for the four seasons of 2025. Table 1 specifies the Landsat data of several sensors. Landsat 8

and 9 thermal infrared sensors (TIRS) datasets contain two TIR bands (bands 10 and 11), band 11 in Landsat 8 having a higher calibration uncertainty. Thus, only TIR band 10 data (100 m resolution) were recommended for the current study (Barsi et al., 2014). These images, were obtained from the USGS Earth Explorer (http://earthexplorer.usgs.gov) for path 168 and row 036. ArcGIS Spatial Analyst software (version 10.8.1) was used to process the data, retrieve LST and MNDWI, it was also used to extract multi values of points to analyze the Correlation between two variables, and SPSS 22 were used for the statistical analysis computation. Four land covers have been used as a sample to explain the nature of correlation (Fig 2).

Table.1 Images used in this study (U.S. Geological Survey [USGS], 2026)

Dataset Type\ Sensor	Type of Data	Acquisition Date	Acquisition Time	Cloud Cover (%)	Spatial Resolution	Band Used	Scene ID
Landsat 9	Raster	2025/01/08	07:33:04 07:33:36	4.15	30 m, 100 m	(3 & 6) to MNDWI + (10) to LST	LC09_L1TP_168036_20250108_20250109_02_T1
Landsat 8	Raster	2025/04/06	07:32:35 07:33:07	8.50	30 m, 100 m		LC08_L1TP_168036_20250406_20250412_02_T1
Landsat 8	Raster	2025/08/12	07:32:59 07:33:30	0.00	30 m, 100 m		LC08_L1TP_168036_20250812_20250821_02_T1
Landsat 8	Raster	2025/10/31	07:33:15 07:33:46	0.05	30 m, 100 m		LC08_L1TP_168036_20251031_20251122_02_T1

Figure. 2 Selected Land cover samples (Esri, 2026)

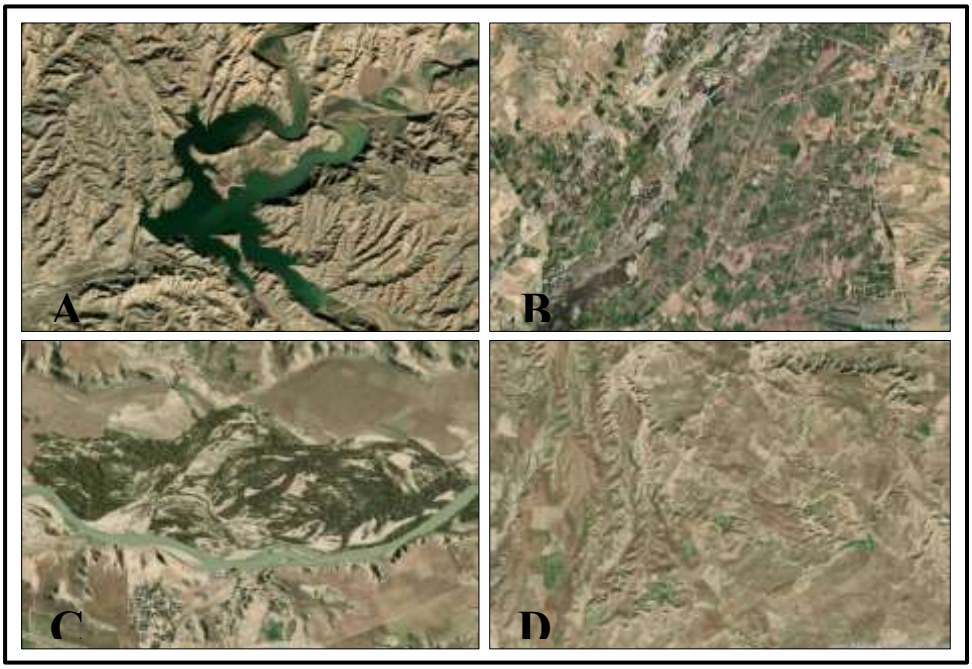

A) Water Body. B) Wet Land. C) Forest. D) Barren Land.

2.3. Methods

2.3.1. Land Surface Temperature (LST) Retrieval

The Mono-Window Algorithm (MW) is a method developed by (Qin et al., 2001) for determining LST using thermal infrared sensor (TIRS) data, particularly from satellite sensors such as the Landsat series. The algorithm is focused on processing the thermal band data to account for air effects and surface emissivity fluctuations, which are critical for accurate LST measurement. In the current work, the MW algorithm was utilized to calculate LST from Landsat 8 and 9 data for the study area. Initially, the thermal band's digital numbers (DN) were transformed to spectral radiance using Equation 1. The spectral radiance was then transformed to brightness temperature by applying Equations 2 and 3. To accurately measure surface emissivity in Landsat images, the proportion of vegetation (Pv) values were

derived from NDVI data, as indicated in Equation 4 and Figure 3. The emissivity of each pixel in the thermal band was then calculated using Equation 5. This thorough technique ensures that both air and surface conditions are adequately accounted for, yielding precise LST estimations (Ahmad & Amin, 2023).

$LST = BT/ (1+(\lambda * BT /p) Ln(\varepsilon))$ (1)

LST: Land Surface Temperature

BT: Satellite brightness temperature

λ: Wavelength of emitted radiance

ε: Surface emissivity for the used channel.

P: is $h \times c/\sigma$ ($1.438 \times 10^{-2}\ m\ K$), where h is Planck's constant ($6.26 \times 10-34 J\ s$); c is the speed of light (2.998×108 m/sec); σ is Stefan Boltzmann's constant ($1.38 \times 10-23 J\ K-1$).

$BT = ((K2/\text{Ln}\ (K1/\ L\lambda +1)) - 273.15$ (2)

K1: Calibration Constant 1 from the meta data.

K2: Calibration Constant 2 from the meta data.

$L\lambda$: Top of Atmosphere Spectral Radiance

$L\lambda = Ml * Qcal + Al$ (3)

Ml: Band-specific multiplicative rescaling factor from the metadata

Q cal: Digital number of a given pixels]

Al: Band-specific multiplicative rescaling factor from the metadata

$Pv = ((NDVI\ -NDVI\ min)/(NDVI\ max - NDVI\ \ min\ ))^{2}$ (4)

NDVI min: NDVI value of fully bare pixels.

NDVI max: NDVI value of completely vegetated pixels.

$\varepsilon = 0.004 + Pv * 0.986$ (5)

0.004: Average emissivity value of bare land

Pv: Proportion of Vegetation

0.986: Values of average emissivity of the vegetated land.

2.3.2. Modified Normalized Differences Water Index (MNDWI) Calculation

McFeeters (1996) introduced the Non-Urban Surface Water Index (Normalized Differences Water Index - NDWI) in 1996 to identify surface associated with wetlands. NDWI aims to maximize water reflectance through green wavelengths, minimize low NIR reflectance from water features, and maximize on high NIR reflectance from plant and soil. Water characteristics have positive values, while plants and soil typically have zero or negative values, resulting in suppression. However, applying the NDWI to water regions with built-up land backgrounds does not provide the predicted results. The retrieved water information in such places was frequently intermingled with land noise. Many built-up land characteristics contribute positively to the NDWI image. As a result, the computation of the NDWI yields a positive number for both built-up land and water. As a result, the increased water presence in the NDWI image is frequently accompanied by accumulated land noise (Xu, 2006, Ali et al., 2019) Similarly, these results were observed in our study area. Xu (2005) Modified Normalized Differences Water Index (MNDWI) is used to examine the water's composition. It is a crucial indicator for monitoring water stress, drought, soil erosion etc. By using the green (GREEN) and the short-wave infrared (SWIR) bands, its values range from -1 to +1. Low values indicate low water content or low water depth, while high values indicate higher water content or high-water depth (Szabó et al., 2016).

$$\text{MNDWI} = \frac{(\text{Green} - \text{SWIR 1})}{(\text{Green} + \text{SWIR 1})}$$

SWIR stands for short-wave infrared spectrum, while GREEN is the indication in the green array spectrum. ArcMap 10.8.1 Spatial Analyzer tool used Raster Calculator to perform MNDWI. The band ratios supervised classification is superior in terms of accuracy when considering other classification techniques (Rashid, 2023).

2.3.3. Resampling LST

Image resampling is the process of changing a sampled image from one coordinate structure to another (Patil, 2018). In contemporary statistics, resampling techniques are an essential tool. To get more details about the fitted model, they entail repeatedly selecting samples from a training set and refitting a model of interest on each sample (James et al., 2023). Resampling employs four interpolation methods; Nearest neighbor, Bilinear interpolation, Bicubic interpolation and Basic-splines (B-spline). This study depends on Bilinear interpolation using Arc GIS, to determine its ultimate value, it will take the weighted mean value of the four pixels in the surrounding area. The weighted average of the four pixels closest to the enumerated input coordinates will be used to determine values at the random position, which will then be assigned to the output coordinates. This method interpolates in both vertical and horizontal directions. For bilinear interpolation, this is the interpolation kernel.

$$u(x) = \left\{1 - \begin{matrix} 0\,, & |x| > 1 \\ |x|, & |x| < 1 \end{matrix}\right\}$$

The grid point's distance from the interpolated point is indicated by x (Patil, 2018).

2.3.4. Statistical Analysis

A point-based spatial correlation analysis was carried out to investigate the relationship between land surface temperature and moisture availability. In particular, a grid of sample locations was created throughout the study areas various land surfaces. The pixel values for the Modified Normalized Difference Water Index (MNDWI) and Land Surface Temperature (LST) were extracted to each point location using a spatial extraction method. Because there was a 1:1 relationship between the variables, Pearson's correlation coefficients could be calculated to determine how strongly and in which direction the variables were associated. This correlation provides standardized measure of linear association between variables, the result ranges from -1 (perfect negative correlation) to +1 (perfect positive correlation) between variables to show the strength of this relationship, and displayed as scatter plot with quantifying this relationship with linear regression. PCC is often used in data analysis and statistics to identify correlations between variables. In invariant fields, it is particularly useful for assessing the strength and direction of interactions between different elements or variables (Amin et al., 2024). The Pearson correlation coefficient can be calculated using the following formula (Ahlgren et al., 2003):

$$r = \frac{\sum(xi - \bar{x})(yi - \bar{y})}{\sqrt{\sum(xi - x)^2}\sqrt{\sum(yi - \bar{y})^2}}$$

r: Pearson correlation coefficient

xi: Value of the first variable (x) for the i-th data point
yi: Value of the second variable (y) for the i-th data point
$\bar{x}$: Mean (average) of the x values
$\bar{y}$: Mean (average) of the y values

Figure 3. Flowchart shows the methodology

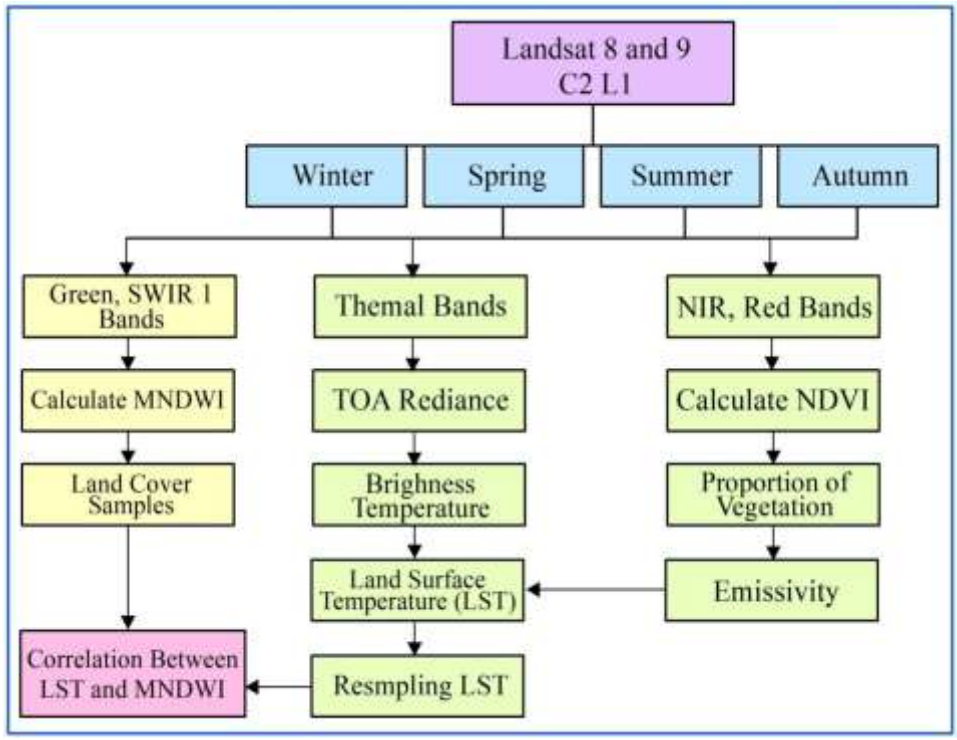

3. Result and Discussion

3.1 Seasonal distribution of LST for different land covers

The LST follows a regular seasonal curve, with noteworthy exceptions in summer and spring. Summer temperatures are exceptionally high, averaging 47.92°C and peaking at 59.19°C. This suggests that the location receives a lot of light and may not have much vegetation cooling. Spring has the highest Standard Deviation (4.32), indicating that it is a "volatile" season, with temperatures wildly varying as the region transitions from winter

cold to summer heat. Winter is rather mild (15.17°C on average), although a minimum of 1.17°C suggests that there may be occasional near-freezing events. Interestingly, Autumn is substantially warmer than Spring (mean: 31.89°C versus 28.06°C). (Table. 2).

Figure 4 . LST map of the study area in different season

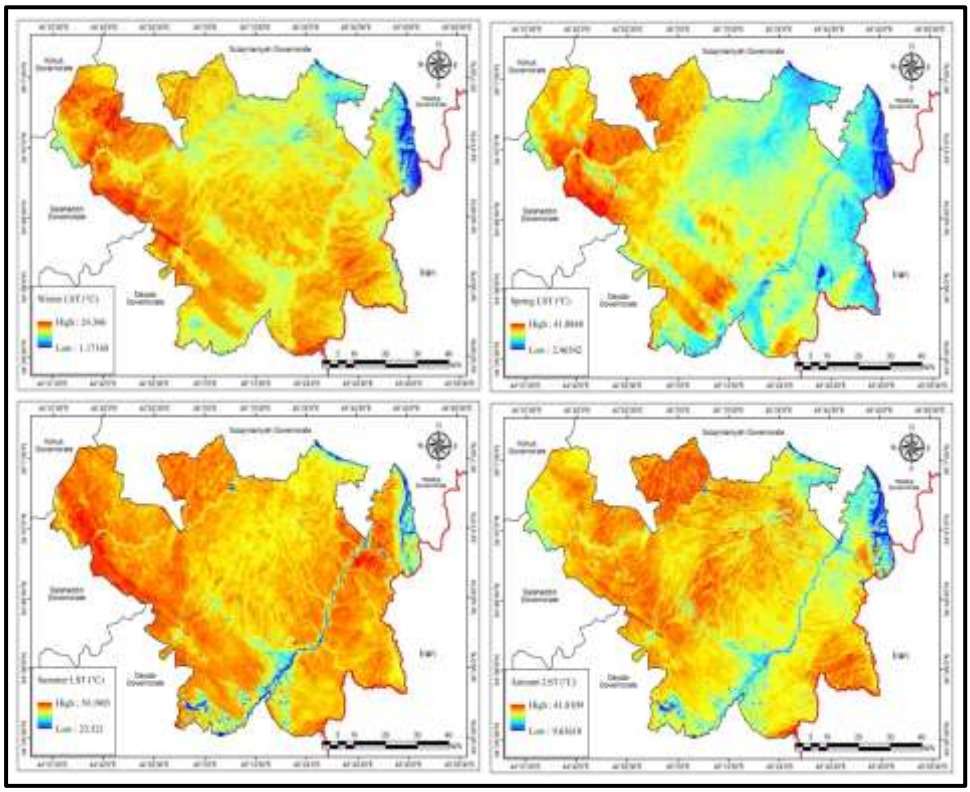

Water bodies provide a cooling impact and continuously maintain the lowest LST across all seasons, peaking at 33.41°C in the summer, whereas Barren Land rises to 49.45°C. This demonstrates the tremendous thermal inertia of water. While barren ground exhibits the most dramatic seasonal variation. The temperature fluctuates by roughly 33°C between winter and summer, most likely due to a lack of vegetative cover to provide shade or evapotranspiration. Wetlands and vegetation have

similar thermal profiles in winter (14°C), but differ slightly in summer. Wetlands are slightly cooler (43.42°C) than forests (38.84°C). Dense forests may be cooler due to canopy effects (Table 3).

3.2 Seasonal distribution of MNDWI for different land covers

MNDWI mean values are negative across all seasons (ranging from -0.14 to -0.20). The values vary by season according to the nature of their climate conditions; in autumn, despite the low mean, it reaches a maximum of 0.61. Winter has the highest mean (-0.14) and a very low standard deviation, indicating that moisture levels are most constant throughout the area during the cold months.

The MNDWI values for Water Body are positive (0.12 to 0.24), whereas the negative values for Forest, Wetland, and Barren land are typical of non-water surfaces (Table 3).

Figure 5. MNDWI Map of the study area in different season

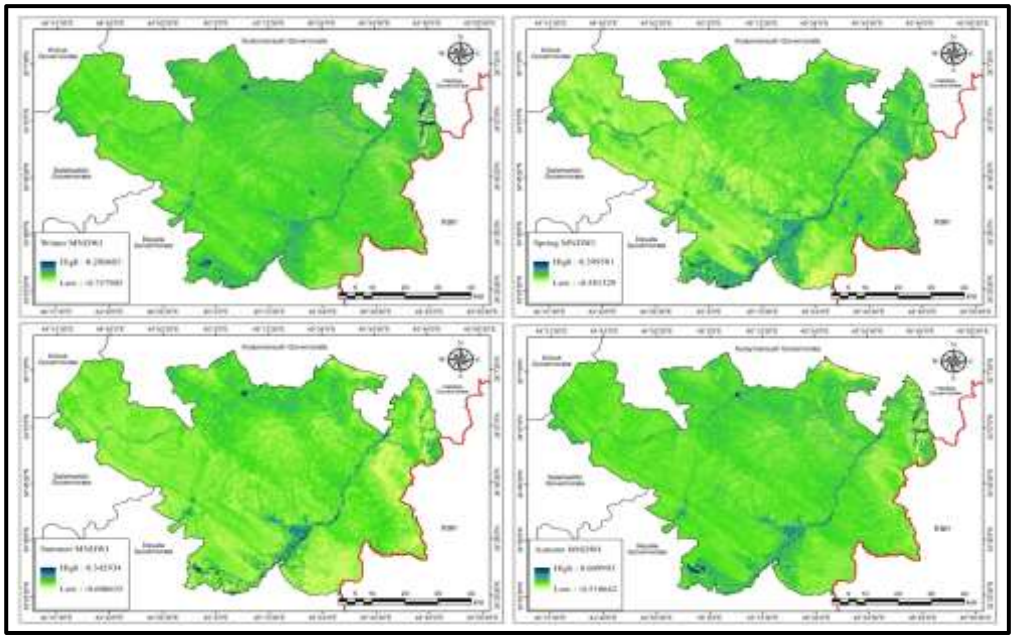

Table.2 Max, min, mean and S.D LST (˚C) and MNDWI value of Garmian administration for the four seasons

Season	Index	Max	Min	Mean	S. D
Winter	LST (˚C)	24.37	1.17	15.17	1.93
	MNDWI	0.28	-0.76	-0.14	0.05
Spring	LST (˚C)	41.08	2.47	28.06	4.32
	MNDWI	0.40	-0.58	-0.17	0.04
Summer	LST (˚C)	59.19	23.52	47.92	2.49
	MNDWI	0.34	-0.61	-0.20	0.03
Autumn	LST (˚C)	41.81	9.64	31.89	2.72
	MNDWI	0.61	-0.51	-0.18	0.04

Table.3 Mean LST (˚C) and MNDWI of Garmian administration of four seasons in different land covers

Season	Index	Water Body	Forest	Wet Land	Barren Land
Winter	LST (˚C)	10.04	14.17	14.13	16.11
	MNDWI	0.14	-0.10	-0.10	-0.13
Spring	LST (˚C)	20.94	23.19	22.86	28.90
	MNDWI	0.24	-0.11	-0.12	-0.17
Summer	LST (˚C)	33.41	38..84	43.42	49.45
	MNDWI	0.12	-0.13	-0.15	-0.19
Autumn	LST (˚C)	23.08	26.28	27.76	31.96
	MNDWI	0.15	-0.11	-0.14	-0.17

3.3 Seasonal Correlation between LST and MNDWI for different land covers

Table 4 demonstrates that the Pearson correlation coefficient (r) is negative in nearly all categories. This demonstrates a negative correlation: the LST falls as the MNDWI rises. The strongest correlation is found between water bodies (r = -0.82) in Autumn, followed by Forest with a value of (r = -0.81) in Summer. Because water takes longer to absorb and release heat, water bodies in the winter have the weakest negative correlation (r = -0.17) and non-significant. The temperature of the surrounding air is sufficiently lower in the winter that the presence of water has less of an impact on the surface temperature than it does in the

summer. Notably, Barren Land has a positive non-significant correlation in the summer (r = +0.17). Regarding the percentage of temperature change (Coefficient of Determination-r^2), moisture levels account for 67% of the temperature variation in Autumn Water Bodies ($r^2 = 0.67$). Moisture explains only 3% of Winter Water Bodies ($r^2 = 0.03$). This implies that LST is influenced by variables other than surface moisture during the winter, such as elevation, solar angle, or wind. In terms of statistical significance (p-value), the majority of p-values are less than 0.01, results suggested that the correlations between LST and MNDWI are statistically significant and very unlikely to be the product of chance excluding winter water body and summer barren land. (Figure 6).

Table 4. Seasonal correlation between LST and MNDWI in different land covers

Season	Land Covers	r	r^2	P. Value
Winter	Water Body	-0.17	0.03	0.23
	Wet Land	-0.53	0.29	0.00
	Forest	-0.25	0.06	0.09
	Barren Land	-0.40	0.16	0.00
Spring	Water Body	-0.61	0.37	0.00
	Wet Land	-0.66	0.44	0.00
	Forest	-0.66	0.44	0.00
	Barren Land	-0.70	0.49	0.00
Summer	Water Body	-0.76	0.58	0.00
	Wet Land	-0.74	0.55	0.00
	Forest	-0.81	0.65	0.00
	Barren Land	+0.١٧	0.٠3	0.٢٥
Autumn	Water Body	-0.82	0.67	0.00
	Wet Land	-0.65	0.43	0.00
	Forest	-0.74	0.54	0.00
	Barren Land	-0.40	0.16	0.00

Our findings are comparable with those of several other studies. Guha and Govil (2025) discovered a negative association between MNDWI and LST, suggesting that water bodies reduce surface temperatures (Guha & Govil, 2025). Chanyal and Purohit (2024) realyzed that NDWI and LST show substantial temporal trends and regional patterns, emphasising the intricate connections between water dynamics and surface temperature in the Kumaun Himalaya. Guha and Govil (2021) studied the NDWI-LST relationship in metropolitan areas and found temperature differences based on proximity to water bodies. Rasul (2016) found that inverse correlation was between LST and moisture surface in Erbil city.

Figure 6. Regression Analysis of LST-MNDWI Correlation for different land covers for different seasons

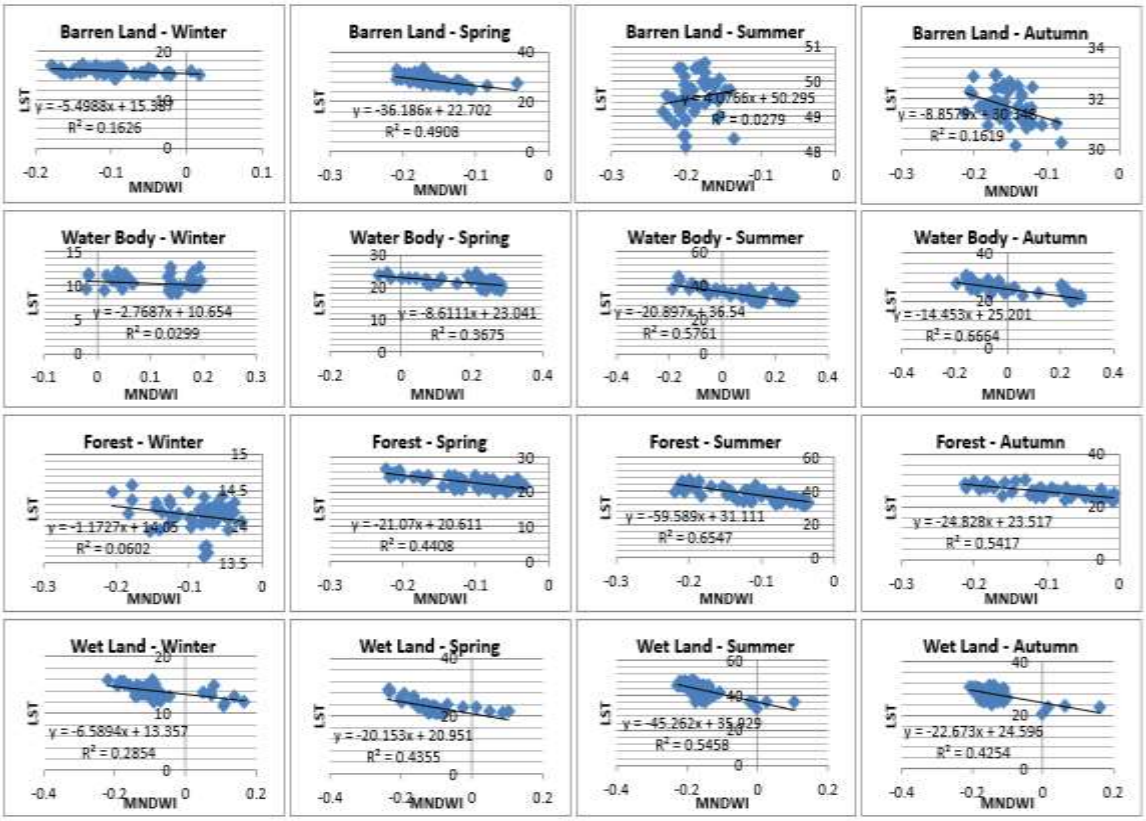

4. Conclusion

This study investigated the seasonal correlation between moisture availability, as measured by the MNDWI and LST, over the Garmian Administration. The key findings revealed that, due to high thermal inertia, water bodies had the lowest LST throughout all seasons and land covers. The maximum LST was in summer with just 33.41°C, and the minimum was in winter with 10.04°C, followed by forest, wet land, and barren land. The greatest and wettest association was noticed in water bodies. Autumn water bodies had the strongest negative correlation (r=-0.82), while Winter water bodies have the smallest (r=-0.17), where other factors may play a greater influence than wetness. MNDWI is a reliable approach for monitoring temperature dynamics in the Garmian area, since most results were statistically significant ($p < 0.01$).

References

- Ahlgren, P., Jarneving, B., & Rousseau, R. (2003). Requirements for a cocitation similarity measure, with special reference to Pearson's correlation coefficient. *Journal of the American Society for Information Science and Technology*, 54(6), 550–560.
- Ahmad, S. H., & Amin, A. H. N. M. (2023). Spatio-temporal variation of the surface urban heat and cool island in Sulaymaniyah City: Land use/cover change implications. *Sulaimani Journal for Humanities*, 25(3), 611–631.
- Ali, A., Hussain, B., Hissan, R. U., Al Aiban, K. M., Radulescu, M., & Magazzino, C. (2025). Examining the landscape transformation and temperature dynamics in Pakistan. *Scientific Reports*, *15*.
- Ali, M. I., Dirawan, G. D., Hasim, A. H., & Abidin, M. R. (2019). Detection of changes in surface water bodies urban area with NDWI and MNDWI methods. *International Journal on Advanced Science, Engineering and Information Technology*, 9(3), 946–951.
- Amin, H. N. M., & Ahmad, S. H. (2024). Assessment of spatial variation of the surface urban heat and cool island in Sulaymaniyah City during the dry season. *Twejer Journal*, 7(3), 1260–1290.
- Amin, H. N. M., Nasir, S. M., & Amin, H. N. M. (2024). Remote sensing-based analysis of LST and NDVI correlation for the coolest and hottest month of 2023 in Khanaqen City. *Raparin Journal of Humanities (RJH)*, 11(5), 898–914.
- Barsi, J. A., Schott, J. R., Hook, S. J., Raqueno, N. G., Markham, B. L., & Radocinski, R. G. (2014). Landsat-8 thermal infrared sensor (TIRS) vicarious radiometric calibration. *Remote Sensing*, 6(11), 11607–11626.
- Buringh, P. (1960). *Soils and soil conditions in Iraq*. Ministry of Agriculture.
- Chanyal, P. C., & Purohit, S. (2024). A geospatial analysis of climate change impacts: Relationship of normalized difference water index (NDWI) and land surface temperature (LST) in Kumaun Himalaya.
- Cui, D., Liang, S., & Wang, D. (2021). Observed and projected changes in global climate zones based on Köppen climate classification. *Wiley Interdisciplinary Reviews: Climate Change*, 12(3), Article e701.

- Esri. (2026). World imagery [Map]. *ArcGIS Desktop (Version 10.8.1)*. https://www.arcgis.com/home/item.html?id=10df2279f9684e4a9f6a7f08febac2a9
- Garmian Administration. (2023). *Map of Residences of Garmian Administration*. Technical Department.
- Ge, X., Mauree, D., Castello, R., & Scartezzini, J. L. (2020). Spatio-temporal relationship between land cover and land surface temperature in urban areas: A case study in Geneva and Paris. *ISPRS International Journal of Geo-Information*, 9(10), 593.
- Grigoras, G., & Uritescu, B. (2024). Analysis of urban thermal environments using satellite data and urban microclimate modeling. *INCAS BULLETIN*, *16*(3), 39–49.
- Guha, S., & Govil, H. (2021). Relationship between land surface temperature and normalized difference water index on various land surfaces: A seasonal analysis. *International Journal of Engineering and Geosciences*, 6(3), 165–173.
- Guha, S., & Govil, H. (2025). An analysis of the relationship of land surface temperature with modified normalized difference water index and normalized difference built-up index in Hyderabad City, India. *South African Journal of Geomatics*, 14(1), 141–155.
- James, G., Witten, D., Hastie, T., Tibshirani, R., & Taylor, J. (2023). Resampling methods. In *An introduction to statistical learning: With applications in Python* (pp. 201–228). Springer International Publishing.
- Jassim, S. Z., & Goff, J. C. (Eds.). (2006). *Geology of Iraq*. Dolin, s.r.o.
- McFeeters, S. K. (1996). The use of the Normalized Difference Water Index (NDWI) in the delineation of open water features. *International Journal of Remote Sensing*, 17(7), 1425–1432.
- Patil, M. S. M. M. (2018). Interpolation techniques in image resampling. *International Journal of Engineering & Technology*, 7(3.34), 567–570.
- Pearsall, H. (2017). Staying cool in the compact city: Vacant land and urban heating in Philadelphia, Pennsylvania. *Applied Geography*, 79, 84–92.

- Qin, Z., Karnieli, A., & Berliner, P. (2001). A mono-window algorithm for retrieving land surface temperature from Landsat TM data and its application to the Israel-Egypt border region. *International Journal of Remote Sensing*, 22(18), 3719–3746.
- Rashid, M. B. (2023). Monitoring of drainage system and waterlogging area in the human-induced Ganges-Brahmaputra tidal delta plain of Bangladesh using MNDWI index. *Heliyon*, 9(6), Article e16823.
- Rasul, A. (2016). *Remote sensing of surface urban cool and heat island dynamics in Erbil, Iraq, between 1992 and 2013* [Doctoral dissertation, University of Leicester]. Figshare.
- Sulaymaniyah Statistical Administration. (2022). Master Plan Department.
- Szabó, S., Gácsi, Z., & Balázs, B. (2016). Specific features of NDVI, NDWI and MNDWI as reflected in land cover categories. *Landscape & Environment*, 10(3-4), 194–202.
- U.S. Geological Survey. (2026). Earth Explorer. https://earthexplorer.usgs.gov
- Xu, H. (2006). Modification of normalised difference water index (NDWI) to enhance open water features in remotely sensed imagery. *International Journal of Remote Sensing*, 27(14), 3025–3033.
- Zhang, J., Ullah, S., Tariq, A., Ahmad, I., & Abbas, M. (2026). Linking urban expansion to thermal stress: Assessing land use transitions, spectral dynamics, and surface temperature in Burewala. *Environmental Monitoring and Assessment*, 198(4), 311.